



NUMERICAL STUDY OF TRANSIENT/STEADY STATE MIXED CONVECTION FLOW IN A VERTICAL CHANNEL WITH RADIATION IMPRESSION

*¹Hussaini A., ²Isah B. Y., ¹Zayyanu S. Y.

¹Sokoto State University, Sokoto

²Usmanu Danfodiyo University, Sokoto

*Corresponding authors' email: abdulahihussaini6@gmail.com

ABSTRACT

In this paper, the hydro magnetic combined-convection flow rate of sticky conducting fluid in the presence of cross magnetic field is considered. Referable to the existence of the radiative heat flux in the energy equation, the mathematical model appears to be highly nonlinear. Hence the essential coupled non-linear partial differential equations were solved with an efficient finite difference scheme and analytical solution of the steady state by the Perturbation method. Computations were performed via flow parametric quantities on velocity, temperature, skin friction, Nusselt number as well as the expression of the fluid buoyancy. The numerical solution of the equations are obtained first selecting the parameters that are involved such as working fluid parameter is chosen as 0.71 and 7.0, thermal radiation parameter $0 \leq R \leq 1.8$ to control finite temperature blow up, the Grashof number corresponds to both external heating/cooling with fixed Reynolds number while other parameters are chosen arbitrary. The results were presented on line graphs. It is interested to report that, radiation parameter, temperature difference parameter assists the velocity and temperature. Furthermore, the result exhibited good agreement with earlier reported studies. The results of this study can be applicable to the field of devices for improving heat transfer efficiency, chemical synthesis, enhancing the performances of micro-electro-mechanical systems and mini-devices, heating and energy generation, designing efficient energy conversion processes, and so on.

Keywords: Hydro-Magnetic, Mixed convection, Temperature difference, Radiation

INTRODUCTION

Heat transfer and fluid flow rate have been subjects of explore for many years due to their applications in modern industries. Fluid flows are captured in many mathematical geometries. Such flows could be laminar or turbulent. Fluid dynamics has so many applications in lubrication industries, gas turbine power plant, polymer technology, food processing industries, plasma power plant, thermal and insulating engineering, MHD power generators etc. These fluid flows are driven either by natural, forced or mixed convection. Mixed convection comes up in several technological and industrial processes e.g., nuclear reactors, chemical processing, thermal insulations, pollution control towers in smart cities etc. The buoyancy forces developed as a result of velocity gradients improve the stream and thermal fields accordingly. Thereto, in mixed convection flows, surface resistance and local heat transmission may be expressively encouraged or condensed in comparing to the purely forced convection case. This ensues in the growth or reduction of heat transfer. Keeping in view the prominence of such study, many investigators (Lavine, 1988, Seth, Mishra, Tripathi, 2018, and Mehmood, Rana, Akbar, and Nadeem, 2018) probed mixed convection flow by taking different aspects of the problem. The study of combined natural and forced convection flow in a parallel-plate vertical channel comes up in many pragmatic engineering applications, including heat exchangers, chemical processing tools, geothermal energy mining, food processing, molding and fusing of manufacturing process, dispersion of chemical contaminations in various processes and in the chemical industry, transport system for heated or cooled fluids and many others Chamkha *et al.* (2017). Theoretic study of such kind of fluid flow is very significant in improvement of these applications. Boundary layer flow in the presence of internal heat generation near a vertical porous plate remains an interesting subject of investigation because of the various engineering applications such as thermal

insulation, rocket engine, geothermal reservoirs, combustion chamber and so on. Crepeau and Clarkson (1997) mathematically analysed the natural convection flow near a vertical plate with internal heat generation. Alam *et al.* (2006) numerically examined the forced convection and mass transfer near a vertical porous wall with the combined effect of thermal diffusion and heat generation. Singh *et al.* (2010) considered the impact of heat generation/absorption on mixed convection stagnation point flow past an isothermal vertical wall imbedded in porous media. Makinde (2012) investigated heat and mass transfer due to MHD mixed convection flow toward a vertical wall imbedded in a porous medium with the combined effect of internal heat generation and thermal radiation. Some literature review related to the current investigation can be demonstrated in references (Uddin *et al.*] 2014, Reddy *et al.* 2017, Lopez *et al.* 2017, Khan *et al.* 2020, Li *et al.* 2019 and Nadeem *et al.* 2019).

At high temperatures, the effect of thermal radiation is very significant since it impresses the heat transfer rate, fluid temperature, and velocity profiles. Similarly, at considerably high temperatures, nonlinear thermal radiation plays a pivotal role in fire science and combustion. Thermal radiation is applied in power generation devices, nuclear plants, gas turbines and so on. Furthermore, thermal radiation is used in regulating the rate of heat in some industries in which the quality of the final product is determined by heat-regulating factors. The radiative effect on magneto hydrodynamics flow on an Eyeing power fluid has been explored by Hayat *et al.* (2013) Mahmoud (2007) considered the implication of thermal radiation on the MHD flow of micro polar fluid past a stretching plate with thermal conductivity. He remarked that the thermal conductivity is directly proportional to the thermal boundary layer thickness. Das (2012) presented horizontal plate with the combined effect of variable fluid properties and thermal radiation. Chamkha (2000) studied the effects of buoyancy and thermal radiation on hydro magnetic flow past

a permeable surface with a heat source/sink. Some recent studies such as references (Singh et al. 2020, Jawad et al. 2021 and Zainal et al. 2020) analysed the importance of thermal radiation over/near different geometries through different approaches.

MATERIALS AND METHODS

Mathematical Analysis

Conceive coupled time-dependent heat transfer by unsteady MHD mixed convective flow of a viscous incompressible and electrically conducting fluid under the influence of transverse magnetic field inside a vertical channel formed by two parallel plates. The distance between the channel walls is H. The channel walls are assumed electrically non-conducting. Utilize a Cartesian co-ordinates system with x-axis vertically upwards along the direction of flow and y-axis perpendicular to it. A uniform magnetic field B_0 acts normal to the plates. The density is assumed to be linearly dependent on temperature buoyancy forces in the equations of motion. The flow is presumed laminar and fully developed. Under the usual Boussinesq approximation, the MHD mixed convective fluid flow governed by the following equations.

$$\frac{\partial u'}{\partial t'} = \nu \frac{\partial^2 u'}{\partial y'^2} + g\beta(T' - T_0) - \frac{\partial p'}{\partial x'} \frac{1}{\rho} \tag{1}$$

$$\frac{\partial T'}{\partial t'} = \left[\frac{\partial^2 T'}{\partial y'^2} - \frac{1}{K} \frac{\partial q_r}{\partial y'} \right] \tag{2}$$

The physical measures employed in the above equations are defined in the nomenclature, thus the initial and boundary conditions to be satisfied are;

$$t' \leq 0 : u' = 0, T' = T_0 \text{ for } 0 \leq y' \leq H \tag{3}$$

$$t' > 0 : \begin{cases} u' = 0, T = T_w \text{ at } y' = 0 \\ u' = 0, T = T_w \text{ at } y' = H \end{cases}$$

Where T_0 is the initial temperature of the fluid and plates, T' is the dimensional temperature of the fluid, α is the thermal diffusivity, K is the thermal conductivity, ρ is the density of the fluid, β , is the coefficient of the thermal expansion and β_0 is the strength of applied magnetic field.

The radiative heat flux q_r can be altered using Roseland diffusion approximation according to references [23–26]

$$q_r = -\frac{4\sigma \partial T'^4}{3k^* \partial y} \tag{4}$$

Nevertheless, Rosseland diffusion estimation is only employed in the analysis of optical thick fluid. However, it has been considered in the study of radiation effect on nuclear explosion according to Agha et al. (2014).

In order to simplify the governing equations of the present problem, we next introduce the non-dimensional flow variables as

$$t = t'v/H^2, y = y'/H, u = u'/U, Pr = \nu/\alpha, Gr = g\beta H^2(T_w - T_0)/\nu U \\ R = 4\sigma_1(T' - T_0)^3/\kappa^*K, p = p'H/\rho\nu U, Re = UH/\nu \tag{5}$$

In terms of these non-dimensional variables, the basic eqns. (1) and (2) can be expressed in the dimensionless form,

$$\frac{\partial u}{\partial t} = \frac{\partial^2 u}{\partial y^2} + \frac{Gr}{Re} \theta - \gamma \tag{6}$$

$$Pr \frac{\partial \theta}{\partial t} = \left[1 + \frac{4}{3} R(C_T + \theta)^3 \right] \frac{\partial^2 \theta}{\partial y^2} + 4R[C_T + \theta]^2 \left(\frac{\partial \theta}{\partial y} \right)^2 \tag{7}$$

Using Eqn. (5) beginning and boundary conditions Eqn. (3) for velocity and temperature field become:

$$t \leq 0 : u = 0, \theta = 0 \text{ for } 0 \leq y \leq 1 \\ t > 0 : \begin{cases} u = 0, \theta = 1 \text{ at } y = 0 \\ u = 0, \theta = 0 \text{ at } y = 1 \end{cases} \tag{8}$$

Approximate Solution

Several methods ranging from numerical, perturbations and many other approximate solution techniques are used to unriddle linear, nonlinear and coupled (partial or ordinary) differential equations. Nevertheless, the analytical solutions have acted a crucial role in verifying and exploring computer routines of complicated problems. For this reason, we reduce the governing equations of this problem into a form that can be solved analytically by fixing $\frac{\partial u}{\partial t} = \frac{\partial \theta}{\partial t} = 0$ to receive the steady state interpretation of the problem.

$$\frac{\partial^2 u}{\partial y^2} + \frac{Gr}{Re} \tag{9}$$

$$\left[1 + \frac{4}{3} R(C_T + \theta)^3 \right] \frac{\partial^2 \theta}{\partial y^2} + 4R[C_T + \theta]^2 \left(\frac{\partial \theta}{\partial y} \right)^2 = 0 \tag{10}$$

With the corresponding condition in dimensionless form as

$$t \leq 0 : u = 0, \theta = 0 \text{ for } 0 \leq y \leq 1 \tag{11}$$

$$t > 0 : \begin{cases} u = 0, \theta = 1 \text{ at } y = 0 \\ u = 0, \theta = 0 \text{ at } y = 1 \end{cases}$$

To concept approximate solutions of equations (9) and (10) subject to (11), we assume a power series expansion in the radiation parameter R of the form subject

$$\begin{cases} u = u_0 + R u_1 \\ \theta = \theta_0 + R \theta_1 \\ \gamma = \gamma_0 + R \gamma_1 \end{cases} \tag{12}$$

Invoking equation (12) into (9)-(11) and comparing the coefficient of like power of R the ensuing solutions of the momentum and energy balance equations are as

$$\frac{d^2 u_0}{dy^2} = -\frac{Gr}{Re_{00}} \tag{13}$$

$$\frac{d^2 u_1}{dy^2} = -\frac{Gr}{Re_{11}} \tag{14}$$

$$\frac{d^2 \theta_0}{dy^2} = 0 \tag{15}$$

$$\frac{d^2 \theta_1}{dy^2} = -\frac{4}{3} [C_T + \theta_0]^3 \frac{d^2 \theta_0}{dy^2} - 4[C_T + \theta_0]^2 \left(\frac{d\theta_0}{dy} \right)^2 \tag{16}$$

And the boundary conditions (11) are transformed as

$$\begin{cases} u_0 = 0, \theta_0 = 1 \text{ at } y = 0 \\ u_0 = 0, \theta_0 = 0 \text{ at } y = 1 \\ u_1 = 0, \theta_1 = 0 \text{ at } y = 0 \\ u_1 = 0, \theta_1 = 0 \text{ at } y = 1 \end{cases} \tag{17}$$

Figuring out from the above equations (13), (14), (15) and (16) and employing the boundary conditions (17), we obtain momentum and energy equations as follows

$$\theta_0(y) = 1 - y \tag{18}$$

$$\theta_1(y) = 2B^2(y - y^2) - \frac{4B}{3}(y - y^3) + \frac{1}{3}(y - y^4) \tag{19}$$

$$u_0(y) = -\frac{Gr}{Re} \left[\frac{1}{2}(y - y^2) - \frac{1}{6}(y - y^3) \right] + \frac{\gamma_0}{2} [y^2 - y] \tag{20}$$

$$u_1(y) = -\frac{Gr}{Re} \left\{ \left[2B^2 - \frac{4B}{3} + \frac{1}{3} \right] \left(\frac{y - y^3}{6} \right) - \frac{B^2}{6}(y - y^4) + \frac{B}{15} \left(\frac{y - y^5}{6} \right) - \frac{1}{90}(y - y^6) \right\} + \frac{\gamma_1}{2}(y^2 - y) \tag{21}$$

$$\left. \begin{aligned} \int_0^1 u_0(y) dy &= 1 \\ \int_0^1 u_1(y) dy &= 0 \end{aligned} \right\} \quad (22)$$

The pressure terms γ_0 and γ_1 in equation (20) and (21) are determined using the expressions (22) to obtain

$$\gamma_0 = -12 + \frac{Gr}{2Re} \quad (23)$$

$$\gamma_1 = \frac{Gr}{Re} \left[\frac{6B^2 - 4B + 1}{6} - \frac{3B^2}{5} + \frac{12B}{45} - \frac{1}{21} \right] \quad (24)$$

Furthermore, the steady state skin friction on the boundaries $y = 0$ and $y = 1$ is:

$$\tau_0 = \left. \frac{du_0}{dy} \right|_{y=1} = \frac{1}{12} \frac{Gr}{Re} - 6 \quad (25)$$

$$\tau_1 = \left. \frac{du_1}{dy} \right|_{y=1} = \frac{1}{12} \frac{Gr}{Re} - 6 + RA_3 \quad (26)$$

Lastly the expressions for the buoyancy critical value at $y = 0$ and $y = 1$ are

$$\left. \frac{Gr}{Re} \right|_{y=0} = - \frac{[6 + RK_5]}{12} \quad (27)$$

$$\left. \frac{Gr}{Re} \right|_{y=1} = \frac{72}{[1 + 12RA_3]} \quad (28)$$

RESULTS AND DISCUSSION

Numerical Solution

The momentum and energy equations given in Equations (9) and (10) are solved numerically using implicit finite difference method as the technique is always convergent and unconditionally stable. Since the values of u and θ at grid point $t = 0$ are known from the initial and boundary conditions. Forward difference is expended for all time derivatives and approximate both the second and first derivatives with second order central differences.

$$\begin{aligned} & -r_1 u_{i-1}^{j+1} + [1 + 2r_1] u_i^{j+1} - r_1 u_{i+1}^{j+1} \\ & = r_2 u_{i-1}^j + [1 - 2r_2] u_i^j + r_2 u_{i+1}^j + \dots \\ & \frac{\Delta t Gr}{Re} \theta_i^j - \Delta t \left[RA_1 \frac{Gr}{Re} + \frac{Gr}{Re} - 12 \right] \end{aligned} \quad (29)$$

$$\begin{aligned} & -r_1 q_1 \theta_{i-1}^{j+1} + [1 + 2r_1 q_1] \theta_i^{j+1} - r_1 q_1 \theta_{i+1}^{j+1} \\ & = r_2 q_1 \theta_{i-1}^j + [1 - 2r_2 q_1] \theta_i^j + \dots \\ & r_2 q_1 \theta_{i+1}^j + \frac{\Delta t R}{(dy)^2} [C_T + \theta_i^j]^2 (\theta_{i+1}^j - \theta_{i-1}^j)^2 \end{aligned} \quad (30)$$

Whereas $r_1 = \frac{\alpha \Delta t}{(dy)^2}$, $r_2 = \frac{(1-\alpha)\Delta t}{(dy)^2}$, $q = 1 + \frac{4R}{3} (C_T + \theta_i^j)$ and $0 \leq \alpha \leq 1$.

Validation of Numerical Models

In order to ascertain the validity of our numerical solution, the numerical results are plotted together with analytical solution derived for steady state problem using perturbation technique. The results provide an excellent agreement as transient solution attains maximum time t as depicted in Figure 1.

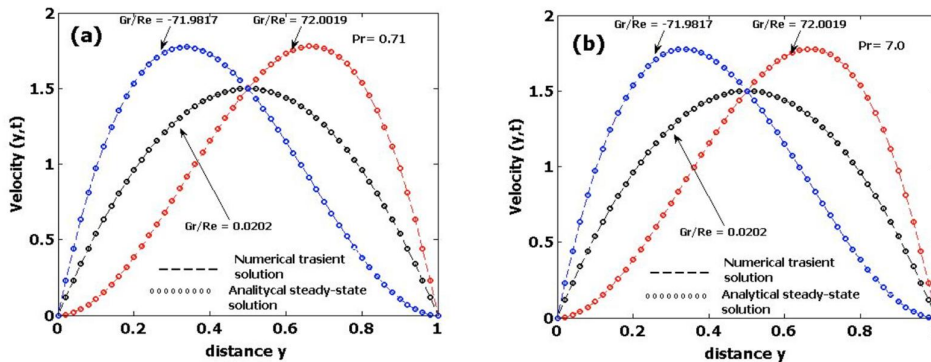


Figure 1: Comparison of transient and steady state velocity profile

Discussion of the Findings

The mixed convection flow from a convective heated vertical plate influenced by nonlinear thermal radiation is explored. The unsteady solutions received in Eqs. (18-28) is seen to be controlled by mixed convection parameter $\left(\frac{Gr}{Re} O\right)$, temperature difference (C_T), Prandtl number ($Pr = 0.71$ and 7.0), radiation parameter (R) and pressure parameter (γ). In order to have a deeper understanding of the present work, MATLAB program is written to compute and generate line graphs for velocity and temperature, skin-friction and Nusselt number at both walls and pressure gradient for different values of governing parameters. The $\left(\frac{Gr}{Re} O\right)$ represents a measure of the effects of the buoyancy in comparison with that of inertia of the external force on fluid flow. Outside the mixed convection region, either the pure forced or the free convection analysis can be used to describe accurately the flow or the temperature field. Forced convection is the dominant mode of transport when $\left(\frac{Gr}{Re} O\right)$, whereas, free convection is the dominant mode when $\left(\frac{Gr}{Re} O\right)$. For the numerical validation of our results, we have chosen physically

meaningful values of the parameters entering the problem. Mixed convection parameter $\left(-71.9857 \leq \frac{Gr}{Re} O\right)$ so that it can capture the occurrence of reverse flow.

Figure 2 (a) and (b) illustrates the relationship in velocity for notable values of fixed convection parameter $\left(\frac{Gr}{Re} O\right)$. It is observed that for fixed value of convective parameter $\left(\frac{Gr}{Re} O\right)$ with varying dimensionless time (t) has been realized to reduce velocity profile but the reverse trend is exhibited for $\left(\frac{Gr}{Re} O\right)$ in air ($Pr = 0.71$). Figures 3 and 4 depict the impact of radiation parameter for fixed values of mixed convection parameter $\frac{Gr}{Re}$ and $\frac{Gr}{Re}$ with two working fluids air ($Pr = 0.71$) and water ($Pr = 7.0$) respectively. It is seen that the advances in the radiation (R) parameter the velocity rises in both working fluid for $\frac{Gr}{Re}$ as shown in Figure 3. Further, in Figure 4 for $\frac{Gr}{Re}$ the velocity decreases with increasing radiation parameter (R). Figure 5 and 6 illustrates the impression of temperature difference (C_T) on velocity profile. It is noticed that in Figure 5(a) that as temperature difference (C_T) grows

the velocity enhances for fixed value of mixed convection parameter $\left(\frac{Gr}{Re}\right)$ in air ($Pr = 0.71$) however, the reverse flow is exhibited in Figure 5(b). Figure 6(a) and (b) on the other hand examines that increase of temperature difference (C_T) decreases velocity profile for fixed value of mixed convection parameter $\frac{Gr}{Re}$ in air ($Pr = 0.71$) and increases in water ($Pr = 7.0$).

The influence of pressure parameter (γ) on the velocity profile is shown in Figure 7(a) and (b). As the pressure parameter extends, it is seen that the velocity profile

increases. It is also revealed that velocity is higher in air ($Pr = 0.71$) in comparison in water ($Pr = 7.0$).

The impact of temperature difference (C_T) on temperature profile is depicted in Figure 8(a) and (b). As the temperature difference (C_T) expands, it is witness that the temperature profile accelerates. Figure 9(a) and (b) present the influence on the temperature profile of the radiation parameter (R). The temperature is detected to heighten as the radiation parameter (R). The reason been due to the reduction in the rate of heat transfer over the surface area.

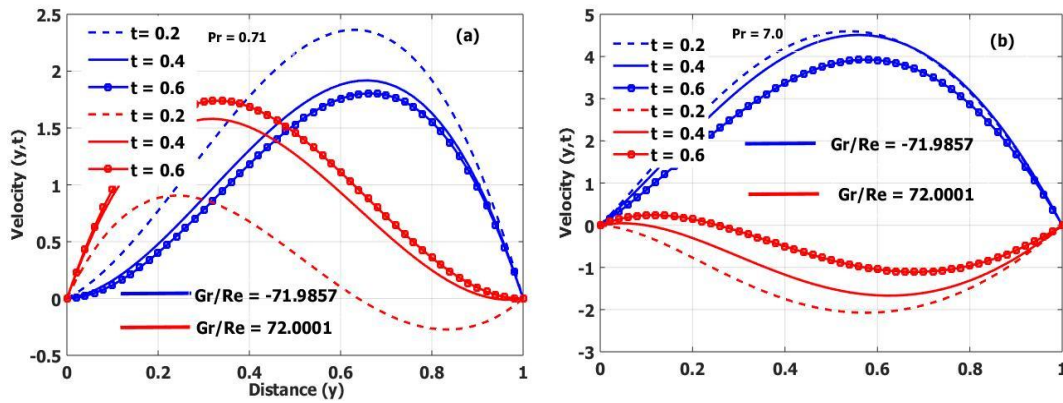


Figure 2: Result of mixed convection parameter on velocity profile

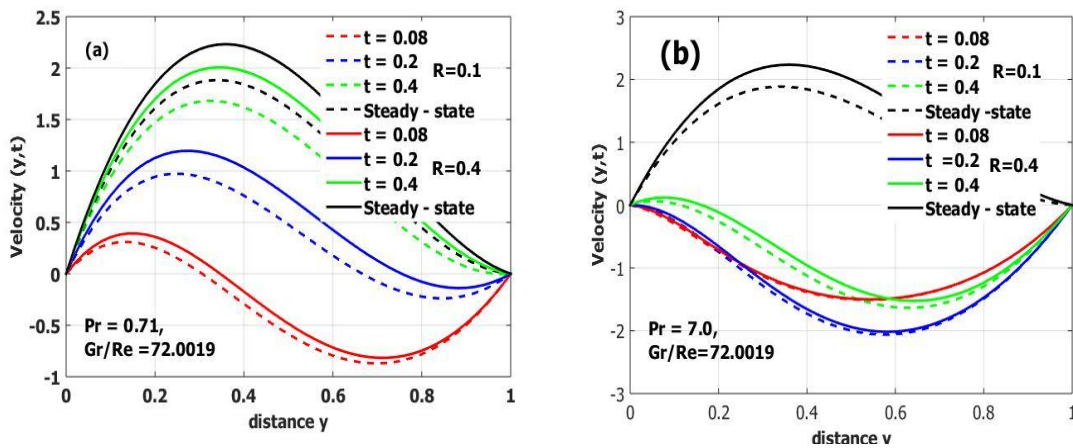


Figure 3: Result of radiation parameter on velocity profile

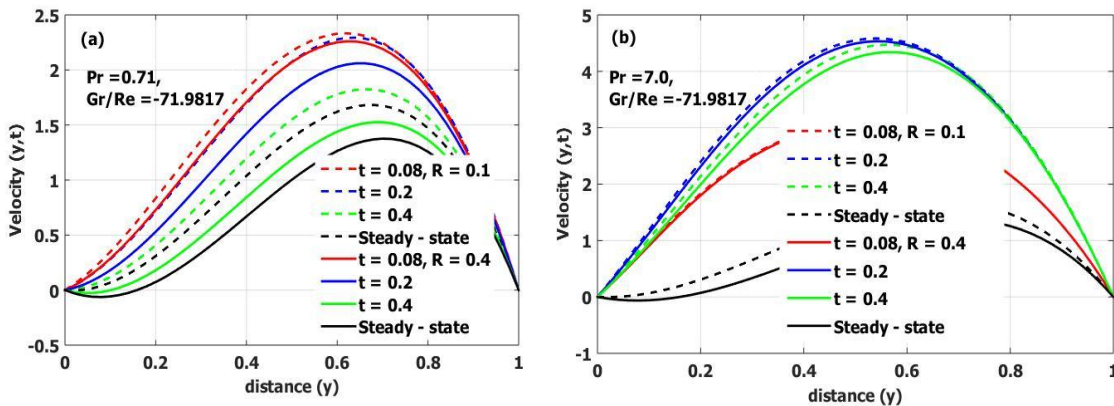


Figure 4: Result of radiation parameter on velocity profile

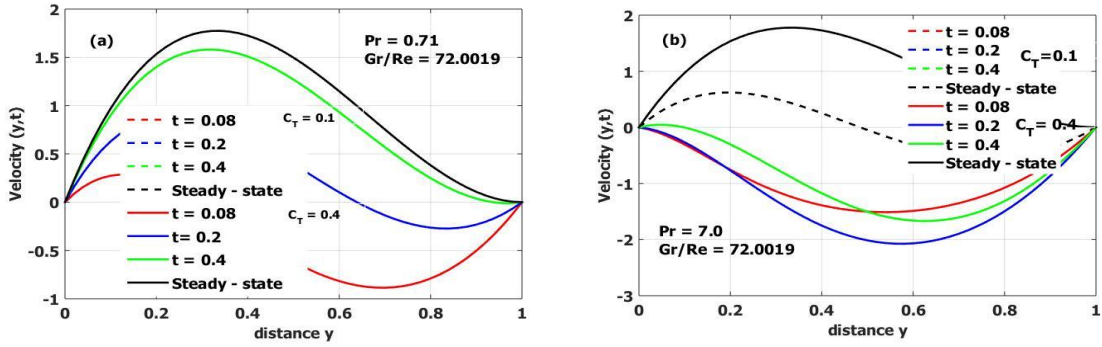


Figure 5: Result of temperature difference parameter on velocity profile

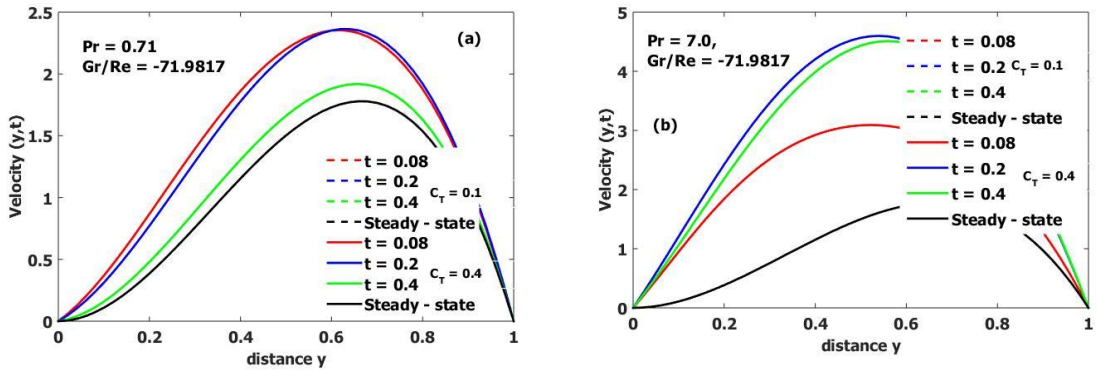


Figure 6: Result of temperature difference parameter on velocity

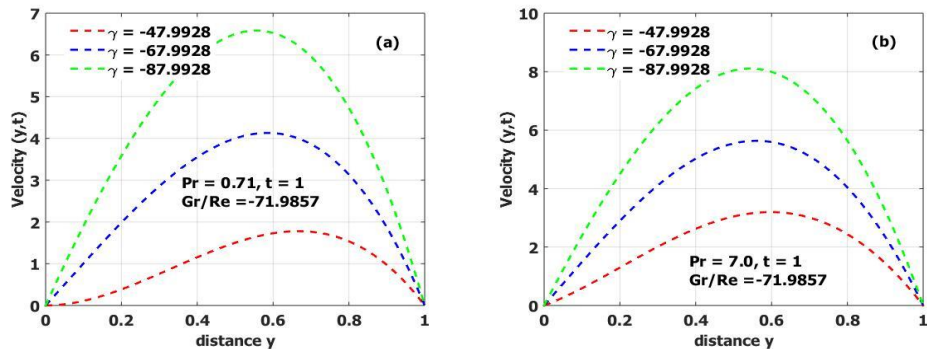


Figure 7: Result of pressure parameter on velocity profile

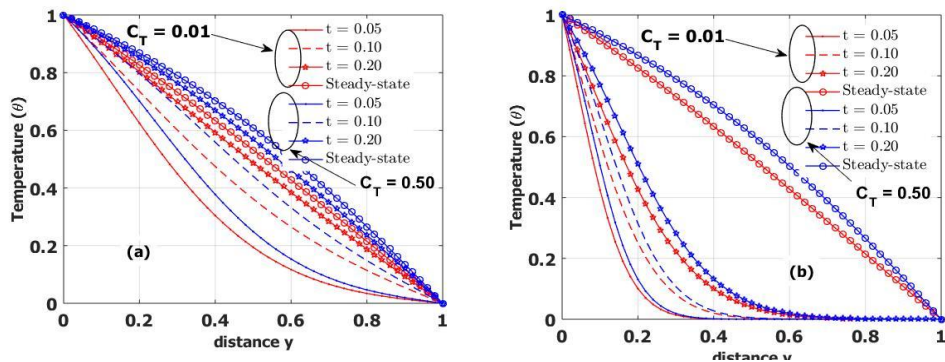


Figure 8: Result of temperature difference parameter on temperature profile

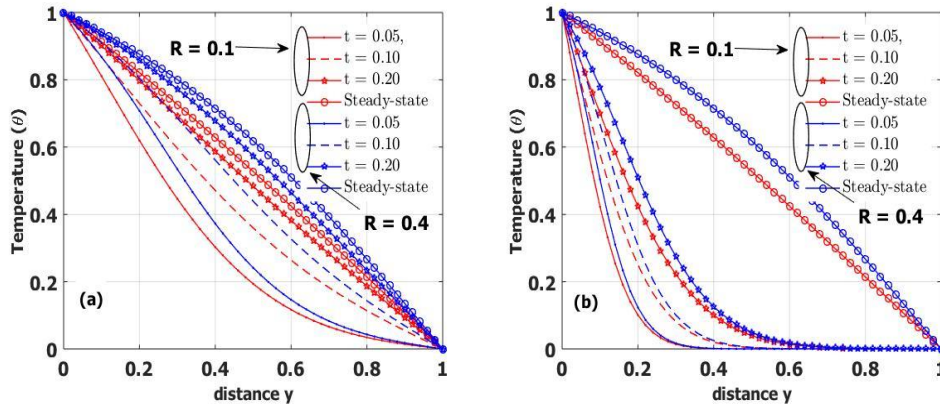


Figure 9: Result of radiation parameter on temperature profile

The impact of dimensionless time (t) with reference to radiation parameter (R) is indicated in Figure 10(a) and (b). It is noticed that as the dimensionless time (t) increases the skin friction is observed to be decelerating. It is also determined that as the radiation parameter (R) increases the skin friction also grows at both plates $y = 0$ and $y = 1$. The variation of dimensionless time (t) with respect to temperature difference (C_T) is examined in Figure 11. It is concluded that as value dimensionless time (t) increases, the skin friction is known to be increasing. It is further realized that for constant value of dimensionless time (t), an insignificant drop is found for values of temperature difference (C_T).

Figure 12 highlights the effect of dimensionless time (t) with reference to radiation parameter (R). It is observed that as the dimensionless time (t) increases, the Nusselt number (Nu) decreases at the plate $y = 0$ and increases at $y = 1$. Variation of dimensionless time (t) with reference to temperature difference is plotted in Figure 13. It is observed that as dimensionless time (t) increases for constant value of temperature difference (C_T), the Nusselt number (Nu) is seen to be decreasing. It is further comprehended that for constant values of dimensionless time (t), as Nusselt number (Nu) increases, temperature difference also decreases at the plate $y = 0$ but exhibited an increase at $y = 1$.

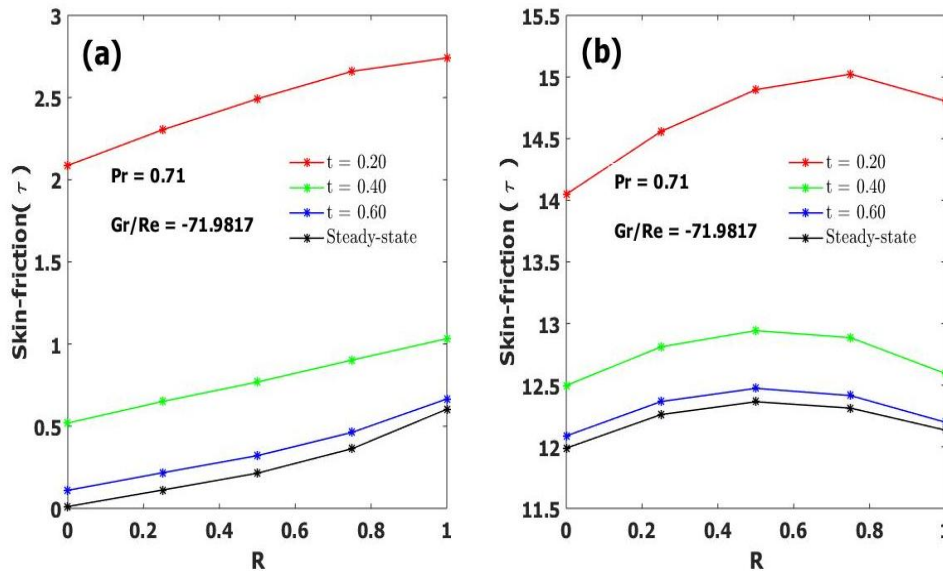


Figure 10: Skin friction for unsteady state at $y = 0$ and $y = 1$

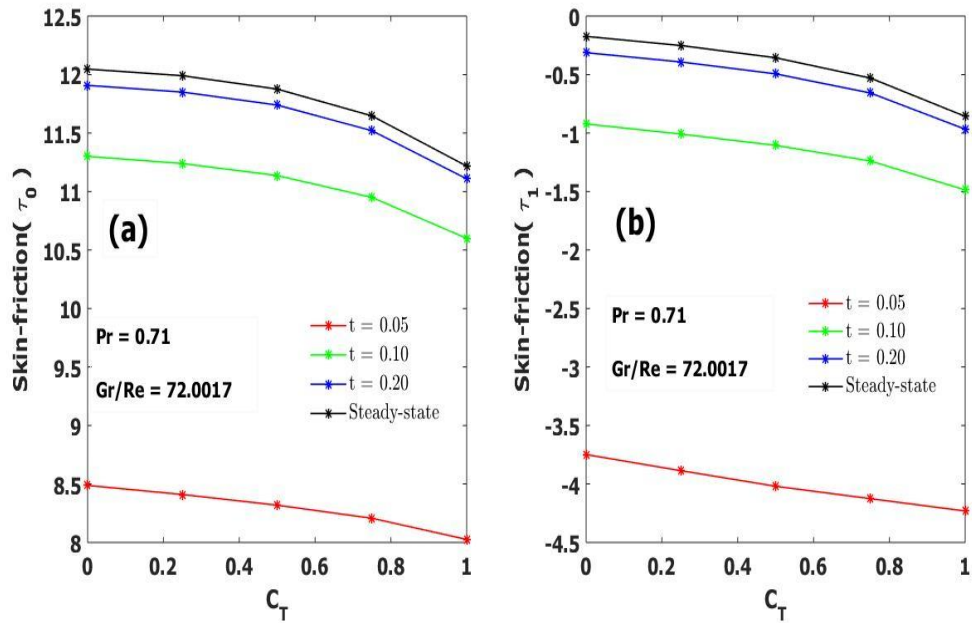


Figure 11: Skin friction for unsteady state at $y = 0$ and $y = 1$

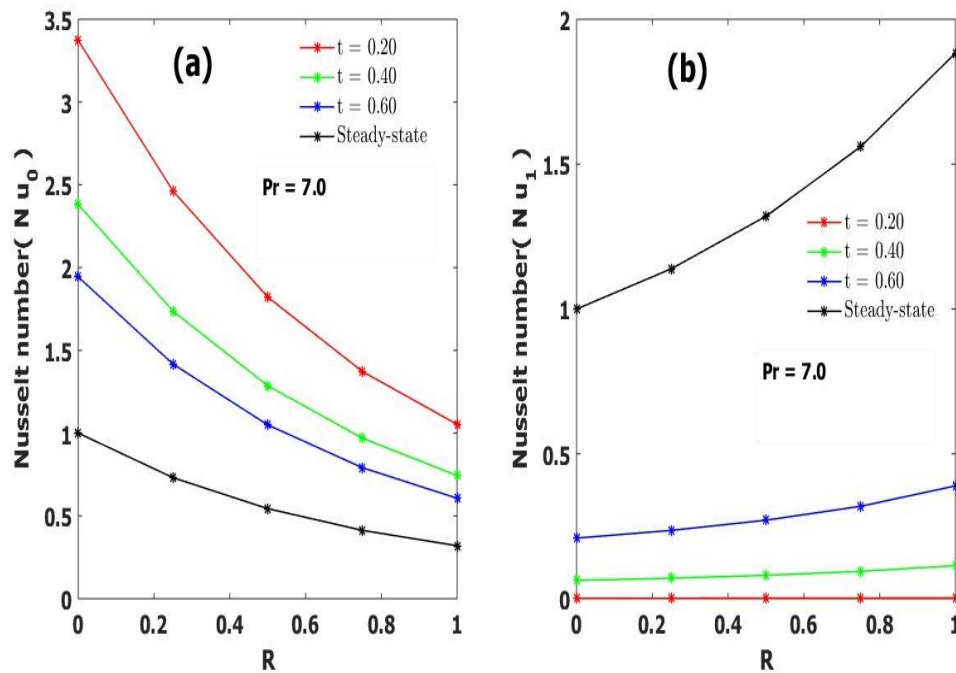


Figure 12: Nusselt number for unsteady state at $y = 0$ and $y = 1$

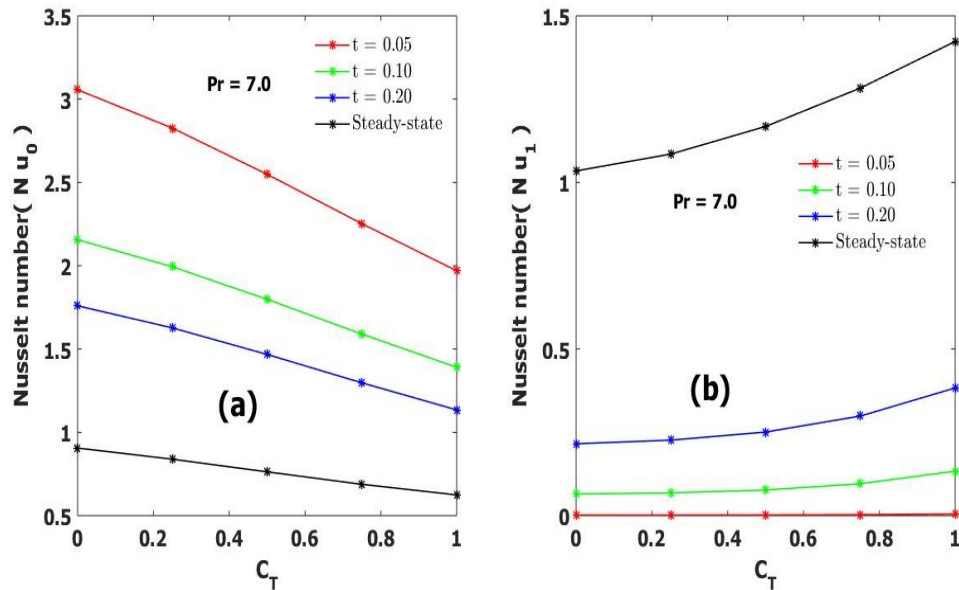


Figure 13: Nusselt number for unsteady state at $y = 0$ and $y = 1$

CONCLUSION

The manuscript investigated the numerical simulation of transient/steady state mixed convection flow in a vertical channel, giving careful thought to some pertinent physical parameters such as radiation parameter, temperature difference parameter, mixed convection parameter, pressure parameter and Prandtl number. The solution of the governing problem for the velocity and temperature fields was investigated analytically using perturbation technique and numerically by finite difference technique. From the analysis following conclusions are arrived at:

- i. Velocity increases for positive values of mixed convection parameter $\left(\frac{Gr}{Re} \theta\right)$ and decreases for negative values $\left(\frac{Gr}{Re} \theta\right)$.
- ii. The velocity increases when the radiation parameter R and temperature difference parameter C_T increase.
- iii. The temperature increases when the radiation parameter R and temperature difference parameter C_T increase.
- iv. Skin friction increases against the rise in C_T but decreases in R .
- v. Nusselt number decreases when the radiation parameter R and temperature difference parameter C_T increase.

REFERENCES

Agha, A. H, Bouaziz M. N. and Hanini, S. (2014) Free convection boundary layer flow from a vertical flat plate embedded in a Darcy porous medium filled with a Nano fluid: effects of magnetic field and thermal radiation. *Arab Journal of Science Eng*, 39: 8331–8340.

Alam, M.S, Rahman, M.M. and Samad, M.A. (2006) Numerical study of the combined free-forced convection and mass transfer flow past a vertical porous plate in a porous medium with Heat generation and thermal diffusion. *Nonlinear Anal Model Control*, 11: 331–343.

Aydın, O. and Kaya, A. (2009) MHD Mixed convective heat transfer flow about an inclined plate. *Heat Mass Transfer*, 46: 29.

Chamkha, A.J. (2000) Thermal radiation and buoyancy effects on hydro magnetic flow over an accelerating permeable surface with heat source or sink. *International Journal of Engineering Science*, 38:1699–1712.

Chamkha, A.J., Rashad, A.M., Mansour, M.A., Armaghani T., and Ghalambaz M. (2017) “Effect of heat sink and source on entropy generation on MHD mixed convection of a Cu-water Nano fluid in a lid-driven square porous enclosure with partial slip. *Phys Fluids*, 29(5): 052001.

Crepeau, J.C. and Clarksean, R. (1997) Similarity solutions of natural convection with internal heat generation. *J Heat Transfer*, 119: 183–185.

Das K. (2012) Impact of thermal radiation on MHD slip flow over a flat plate with variable fluid properties. *Heat Mass Transfer*, 48: 767–778.

Hayat T, Awais M and Asghar S. (2013) Radiative effects in a three-dimensional flow of MHD Eyring-Powell fluid. *J Egypt Math Soc*, 21: 379–384.

Jawad M, Saeed A, Khan A, et al. (2021) Unsteady bio convection Darcy-Forchheimer Nano fluid flow through a horizontal channel with impact of magnetic field and thermal radiation. *Heat Transfer*, 50: 3240–3264.

Khan MR, Pan K, Khan, A.U, et al. (2020) Comparative study on heat transfer in CNTs-water nanofluid over a curved surface. *Int Commun Heat Mass Transfer*, 116: 104707.

Lavine AS. (1988). Analysis of fully developed opposing mixed convection between inclined parallel plates. *Warme fund Stoffübertragung*. Springer, Berlin 23: 249- 257.

Li X, Khan AU, Khan MR, et al. Oblique stagnation point flow of nanofluids over stretching/shrinking sheet with

- Cattaneo-Christov heat flux model: existence of dual solution. *Symmetry (Basel)* 2019; 11: 1070.
- Lopez A, Ibanez G, Pantoja J, et al. Entropy generation analysis of MHD nanofluid flow in a porous vertical microchannel with nonlinear thermal radiation, slip flow and convective-radiative boundary conditions. *Int J Heat Mass Transf* 2017; 107: 982–994.
- Mahmoud, M.A.A. (2007) Thermal radiation effects on MHD flow of a micro polar fluid over a stretching surface with variable thermal conductivity. *Phys A Stat Mech Appl*, 375: 401–410.
- Makinde, O.D. (2012) Heat and mass transfer by MHD mixed convection stagnation point flow toward a vertical plate embedded in a highly porous medium with radiation and internal heat generation. *Meccanica*; 47: 1173–1184.
- Mehmood, R., Rana, S., Akbar, N.S., Nadeem, S. (2018) “Non-aligned stagnation point flow of radiating Casson fluid over a stretching surface. *Alex. Eng. Journal*, 57(2); 939-46.
- Nadeem S, Khan MR and Khan AU. (2019) MHD Stagnation point flow of viscous nanofluid over a curved surface. *Phys Scr*, 94: 115207.
- Rashad AM. (2009) Perturbation analysis of radiative effect on free convection flows in porous medium in the presence of pressure work and viscous dissipation. *Commun Nonlinear Sci Numerical Simulation*, 14: 140–153.
- Reddy CR, Surender O, Rao CV, Adomian decomposition method for Hall and ion-slip effects on mixed convection flow of a chemically reacting Newtonian fluid between parallel plates with heat generation/absorption. *Propuls Power Res* 2017; 6: 296–306.
- Seth, G.S., Mishra, M.K., and Tripathi R. (2018) “Modeling and analysis of mixed convection stagnation point flow of nanofluid towards stretching surface: OHAM and FEM approach. *Computational Applied Mathematics*, 37(4): 4081-103.
- Singh O, Kedare, S.B. and Singh, S. (2020) The validity of approximate boundary conditions for natural convection with thermal radiation in open cavities. *J Heat Transfer*, 142: 092603.
- Singh, G., Sharma, P.R. and Chamkha, A.J. (2010) Effect of volumetric heat generation/absorption on mixed convection stagnation point flow on an iso-thermal vertical plate in porous media. *Int J Ind Math*, 2: 59–71.
- Uddin Z, Kumar M and Harmand S. Influence of thermal radiation and heat generation/absorption on MHD heat transfer flow of a micropolar fluid past a wedge considering hall and ion slip currents. *Therm Sci* 2014; 18: 489–502.
- Zainal, N.A, Nazar, R., and Naganthran, K. (2020) MHD Flow and heat transfer of hybrid Nano fluid over a permeable moving surface in the presence of thermal radiation. *International Journal of Numerical Methods Heat Fluid Flow*, 31: 858–879.



©2024 This is an Open Access article distributed under the terms of the Creative Commons Attribution 4.0 International license viewed via <https://creativecommons.org/licenses/by/4.0/> which permits unrestricted use, distribution, and reproduction in any medium, provided the original work is cited appropriately.